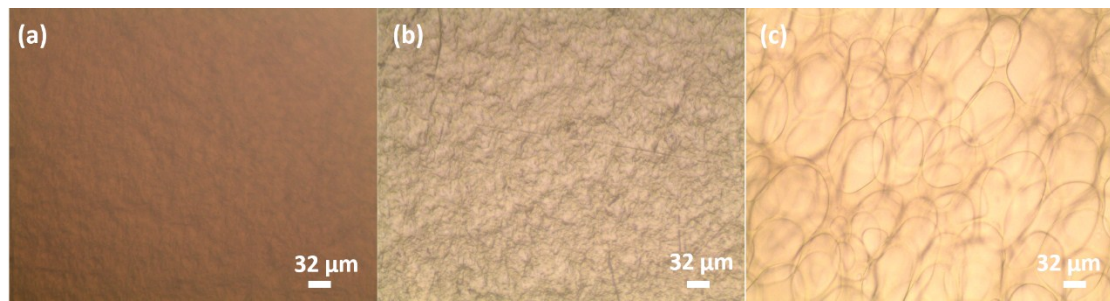


## Supporting Information

**In-situ extracted poly(acrylic acid) contributing to electrospun nanofiber separators with precisely tuned pore structures for ultra-stable lithium-sulfur batteries**

Xiaobo Zhu, Yue Ouyang, Jiawei Chen, Xinguo Zhu, Xiang Luo, Feili Lai, Hui Zhang,  
Yue-E Miao\*, Tianxi Liu



**Fig. S1** Microscope photographs of different electrospinning precursor solutions: (a) PAN, (b) PAA and (c)  $\text{PAN}_6/\text{PAA}_4$ .

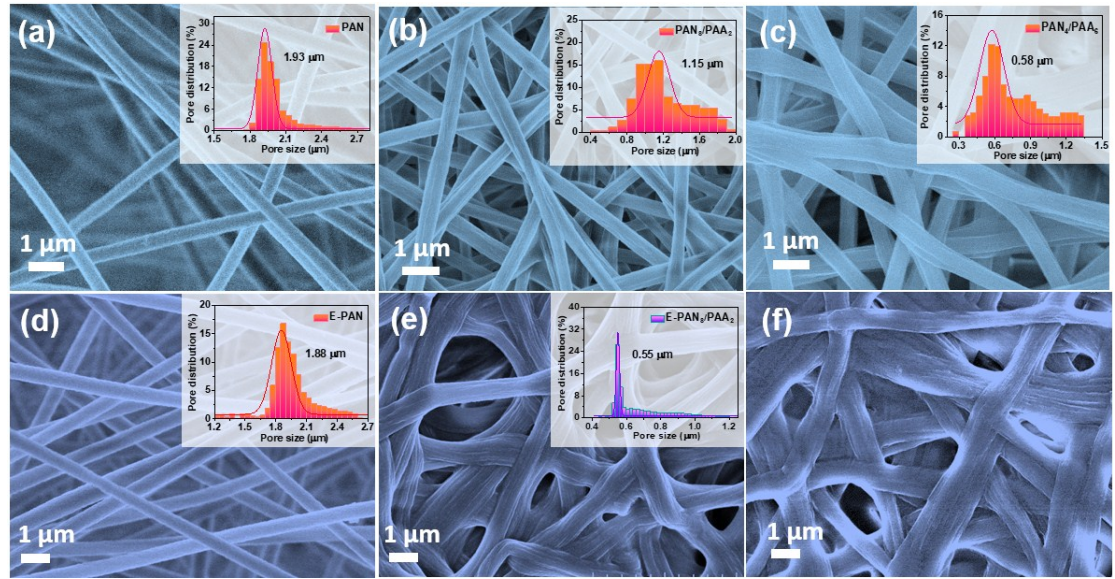


**Fig. S2** SEM images and the corresponding pore size distributions (inset) of different membranes: (a) PAN, (b) PAN<sub>8</sub>/PAA<sub>2</sub>, (c) PAN<sub>4</sub>/PAA<sub>6</sub>, (d) E-PAN, (e) E-PAN<sub>8</sub>/PAA<sub>2</sub>, (f) E-PAN<sub>4</sub>/PAA<sub>6</sub>.

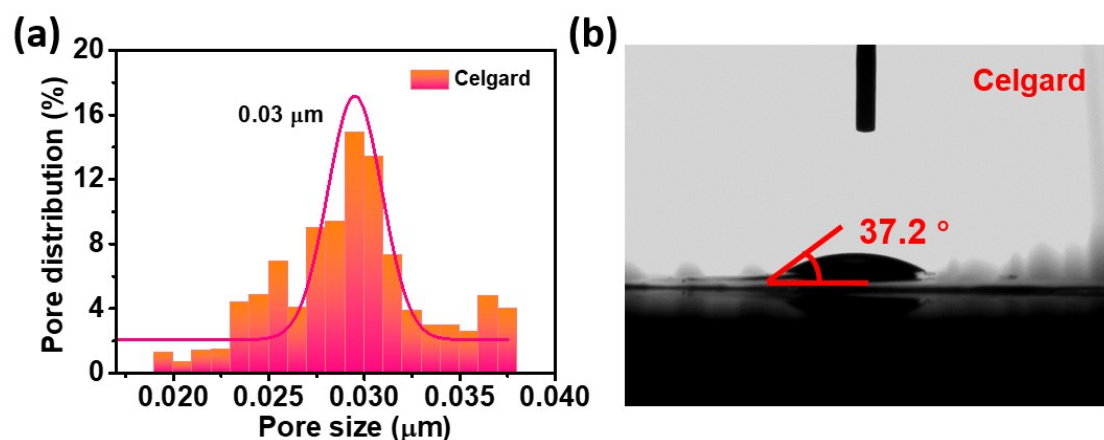


**Fig. S3** (a) The pore size distribution, and (b) electrolyte contact angle of Celgard.

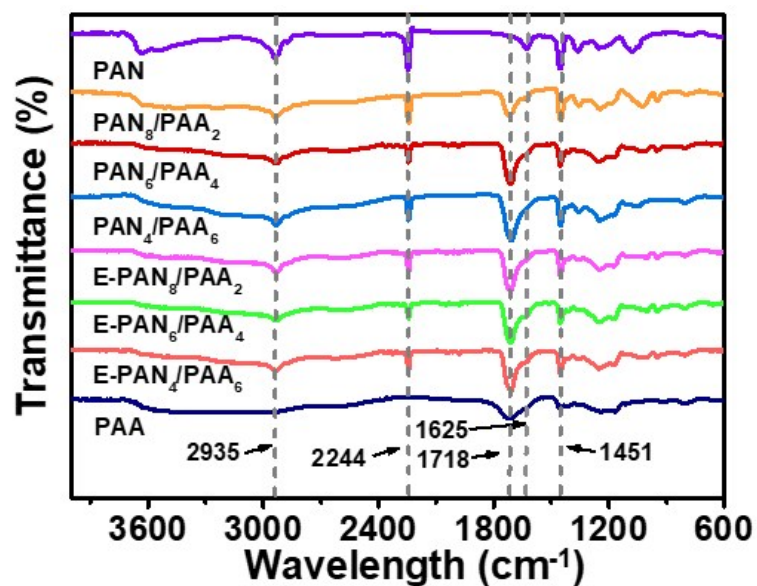


**Fig. S4** FTIR spectra of different membranes.

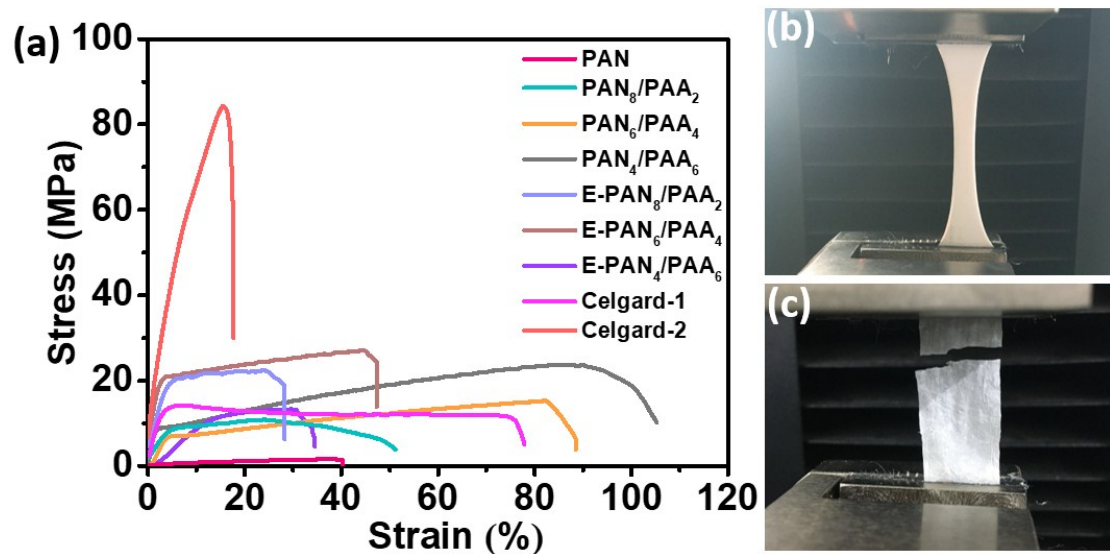


**Fig. S5** (a) Representative stress - strain curves for various membranes. Tensile fracture photos of (b) PAN<sub>6</sub>/PAA<sub>4</sub> and (c) E-PAN<sub>6</sub>/PAA<sub>4</sub> separators.

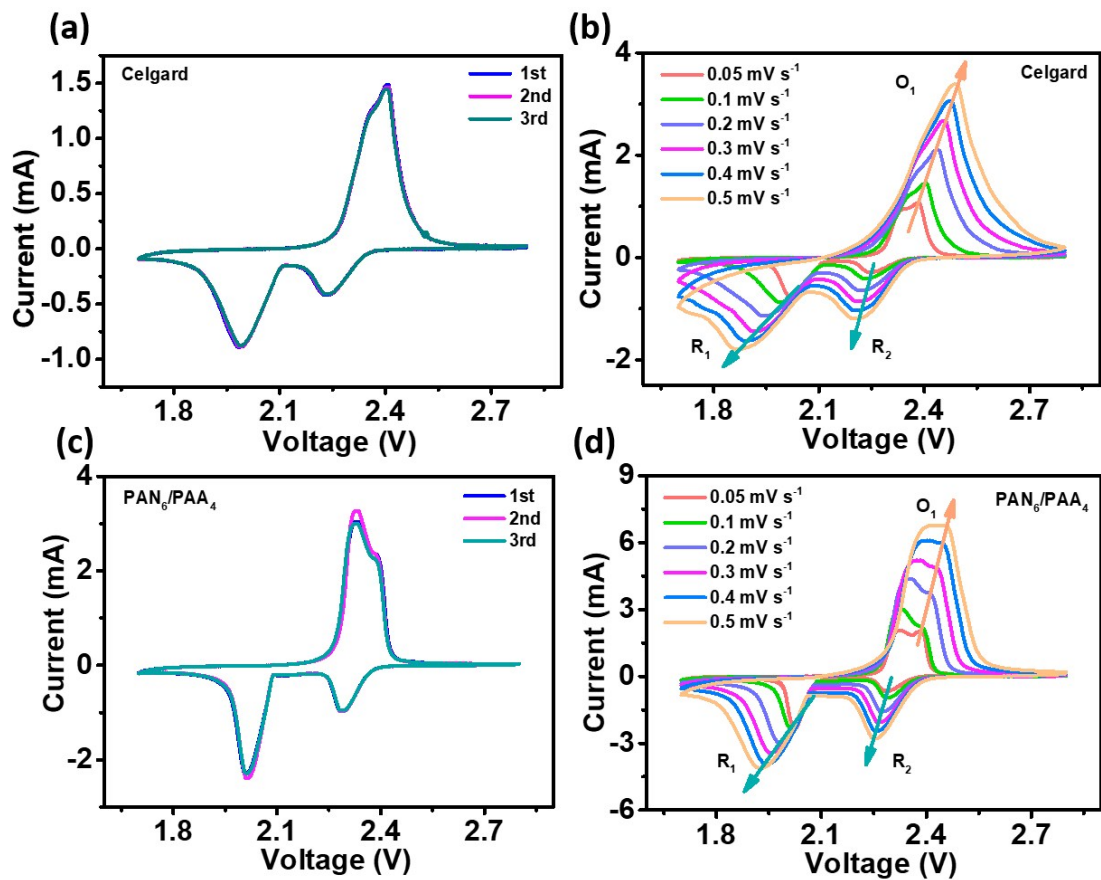


**Fig. S6** CV curves of (a, b) Celgard and (c, d) PAN<sub>6</sub>/PAA<sub>4</sub> separators obtained at a scanning rate of 0.1 mV s<sup>-1</sup> and different scanning rates.

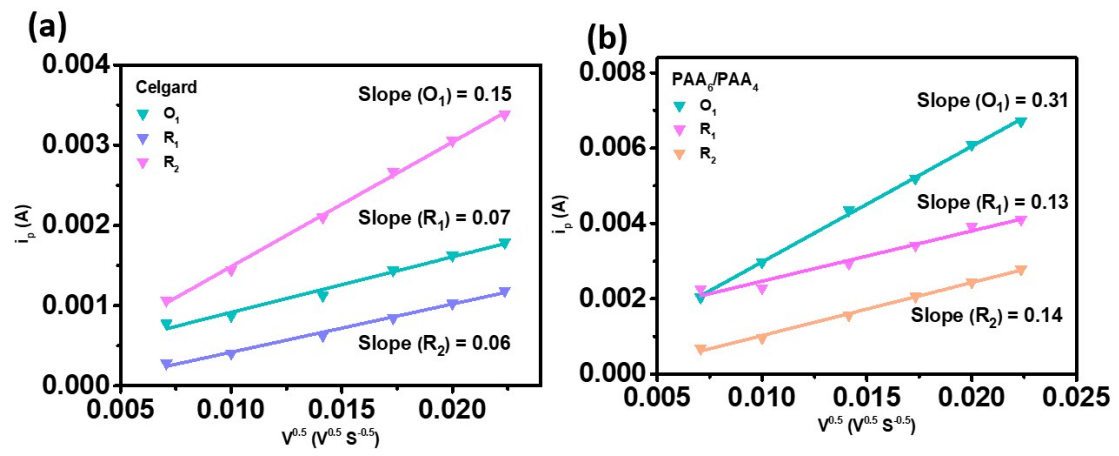


**Fig. S7** Linear fits of the peak currents of Li-S batteries with (a) Celgard and (b)  $PAN_6/PAA_4$  separators.

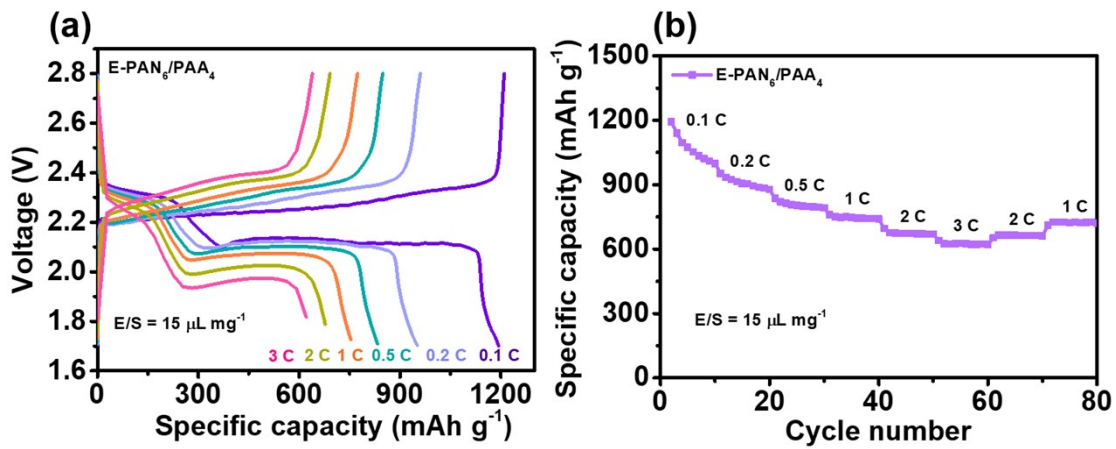


**Fig. S8** Electrochemical performance of the batteries assembled by E-PAN<sub>6</sub>/PAA<sub>4</sub> at a low electrolyte addition (the ratio of electrolyte/sulfur is about 15  $\mu\text{L mg}^{-1}$ ). (a) First cycle discharge/charge curves and (b) rate performance at 0.1, 0.2, 0.5, 1, 2 and 3 C.

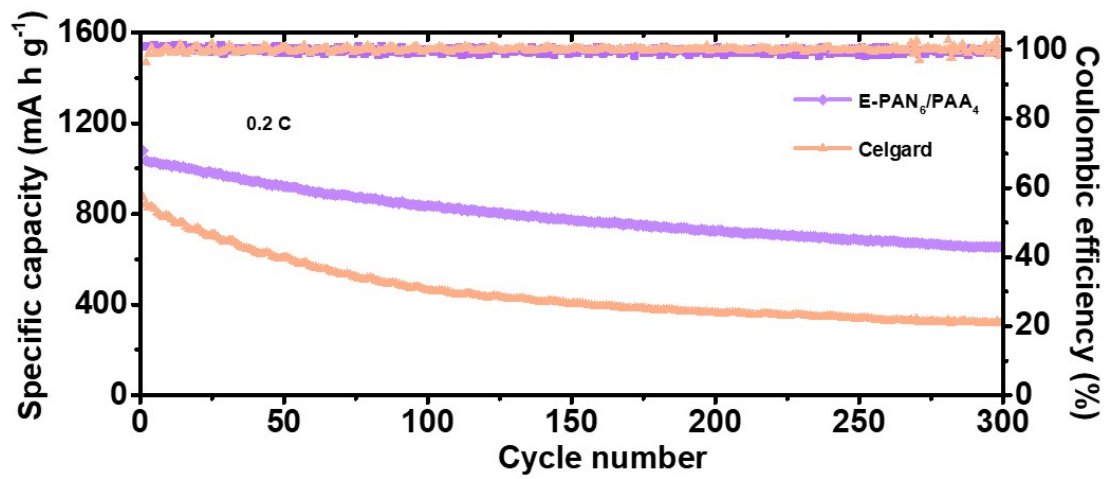


**Fig. S9** The cycling performance of batteries with E-PAN<sub>6</sub>/PAA<sub>4</sub> and Celgard separators at a low rate of 0.2 C.

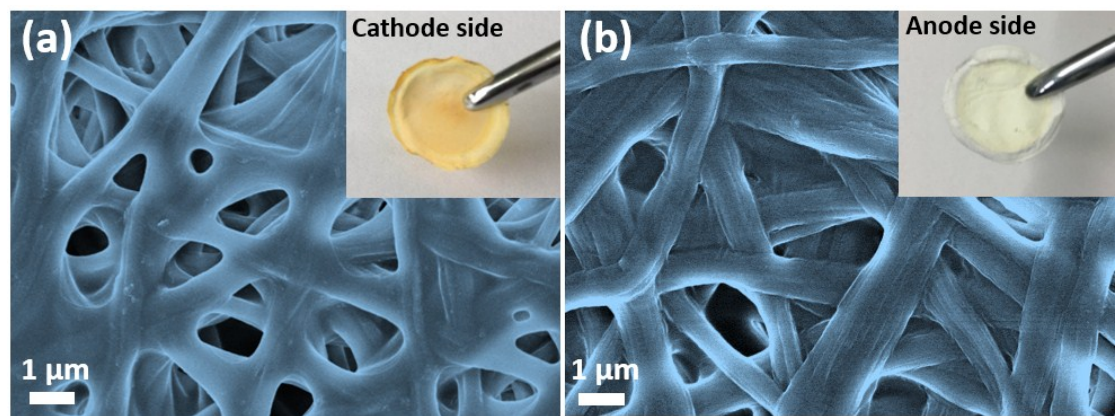


**Fig. S10** SEM images with the corresponding digital photographs (inset) of (a) the cathode side and (b) anode side of E-PAN<sub>6</sub>/PAA<sub>4</sub> separator after 500 cycles of discharge/charge tests.

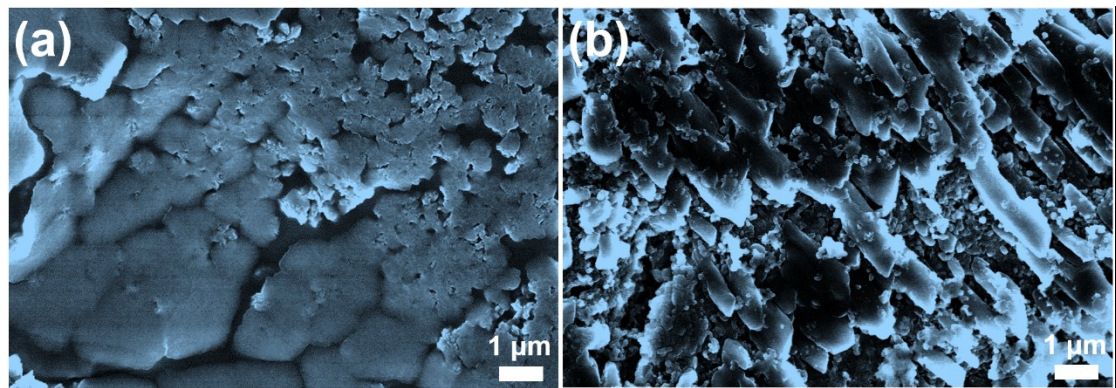


**Fig. S11** SEM images of the Li anodes retrieved from Li-S batteries assembled with (a) E-PAN<sub>6</sub>/PAA<sub>4</sub> and (b) Celgard separators after the cycling test.

**Table S1.** Physical properties of different membranes.

Samples	Thickness ( $\mu\text{m}$ )	Porosity (%)	Density ( $\text{g cm}^{-3}$ )	Contact angle ( $^{\circ}$ )
Celgard	26	40.1	0.57	37.2
PAN	30	91.2	0.16	0
PAN <sub>8</sub> /PAA <sub>2</sub>	32	90.5	0.17	0
PAN <sub>6</sub> /PAA <sub>4</sub>	33	87.3	0.15	0
PAN <sub>4</sub> /PAA <sub>6</sub>	34	83.1	0.16	0
E- PAN <sub>8</sub> /PAA <sub>2</sub>	28	37.1	0.17	0
E- PAN <sub>6</sub> /PAA <sub>4</sub>	30	29.4	0.17	0
E- PAN <sub>4</sub> /PAA <sub>6</sub>	29	19.6	0.19	0

**Table S2.** TGA analyses for different samples.

Samples	The remaining weight ( wt% )
PAN	53.7
PAN <sub>8</sub> /PAA <sub>2</sub>	43.0
PAN <sub>6</sub> /PAA <sub>4</sub>	34.6
PAN <sub>4</sub> /PAA <sub>6</sub>	34.5
E-PAN <sub>8</sub> /PAA <sub>2</sub>	41.2
E-PAN <sub>6</sub> /PAA <sub>4</sub>	34.7
E-PAN <sub>4</sub> /PAA <sub>6</sub>	31.5
PAA	12.5

**Table S3.** Summary of the mechanical properties of different membranes.

Samples	Tensile strength (MPa)	Elongation at break (%)	Young's modulus (MPa)
PAN	1.61 ± 0.27	40.17 ± 4.12	4 ± 1
PAN <sub>8</sub> /PAA <sub>2</sub>	10.88 ± 1.96	53.40 ± 4.31	167 ± 21
PAN <sub>6</sub> /PAA <sub>4</sub>	15.82 ± 1.31	82.22 ± 2.14	485 ± 26
PAN <sub>4</sub> /PAA <sub>6</sub>	23.75 ± 2.19	105.23 ± 2.51	541 ± 43
E-PAN <sub>8</sub> /PAA <sub>2</sub>	22.41 ± 3.07	28.24 ± 1.78	396 ± 34
E-PAN <sub>6</sub> /PAA <sub>4</sub>	27.17 ± 3.36	47.33 ± 1.59	637 ± 63
E-PAN <sub>4</sub> /PAA <sub>6</sub>	13.28 ± 1.34	34.50 ± 1.34	95 ± 32
Celgard-1	14.09 ± 2.16	78.64 ± 4.87	485 ± 47
Celgard-2	84.34 ± 4.12	18.44 ± 1.86	642 ± 69

**Table S4.** Fitted values for the equivalent circuit elements of the electrochemical impedance spectroscopy.

Parameters	$R_0$ ( $\Omega$ )	$R_{ct}$ ( $\Omega$ )	$R_{sf}$ ( $\Omega$ )
PAN	3.5	3.9	~
PAN <sub>8</sub> /PAA <sub>2</sub>	4.9	7.2	2.7
PAN <sub>6</sub> /PAA <sub>4</sub>	6.5	8.4	13.2
PAN <sub>4</sub> /PAA <sub>6</sub>	5.0	11.4	9.7
E-PAN <sub>8</sub> /PAA <sub>2</sub>	14.4	23.8	13.6
E-PAN <sub>6</sub> /PAA <sub>4</sub>	15.6	32.7	15.7
E-PAN <sub>4</sub> /PAA <sub>6</sub>	33.1	44.2	19.3
Celgard	8.7	12.4	14.4

**Table S5.** Summary of the Li<sup>+</sup> diffusion coefficient ( $D_{Li^+}$ ) for Celgard, PAN<sub>6</sub>/PAA<sub>4</sub> and E-PAN<sub>6</sub>/PAA<sub>4</sub> separators.

Parameters	Celgard	PAN <sub>6</sub> /PAA <sub>4</sub>	E-PAN <sub>6</sub> /PAA <sub>4</sub>
$D_{Li^+}$ at peak R <sub>1</sub> (cm <sup>2</sup> s <sup>-1</sup> )	$6.62 \times 10^{-15}$	$2.28 \times 10^{-14}$	$8.65 \times 10^{-15}$
$D_{Li^+}$ at peak R <sub>2</sub> (cm <sup>2</sup> s <sup>-1</sup> )	$4.87 \times 10^{-15}$	$2.65 \times 10^{-14}$	$4.87 \times 10^{-15}$
$D_{Li^+}$ at peak O <sub>1</sub> (cm <sup>2</sup> s <sup>-1</sup> )	$3.04 \times 10^{-14}$	$1.30 \times 10^{-13}$	$3.46 \times 10^{-14}$

**Table S6.** Comparison of the electrochemical performance of this work with previous works involving different separators using carbon-sulfur cathodes in Li-S batteries.

Separator	Sulfur (%)	Initial capacity (mA h g <sup>-1</sup> )	Rate capability (mA h g <sup>-1</sup> )	Fading rate per cycle (%)	Refs
MoS <sub>2</sub> /Celgard	65	1471 (0.1 C)	550 (1 C)	0.08 (0.5 C, 600 cycles)	1
Black phosphorus/Celgard	80	930 (0.4 A g <sup>-1</sup> )	623 (3.5 A g <sup>-1</sup> )	0.14 (0.4 A g <sup>-1</sup> , 100 cycles)	2
KB@Ir/Celgard <sup>a</sup>	75	1600 (0.1 C)	653 (2 C)	0.11 (1 C, 500 cycles)	3
Janus cation exchange membranes	60	1227 (0.05 C)	610 (2 C)	0.24 (0.2 C, 100 cycles)	4
Graphene/polypropylene/Al <sub>2</sub> O <sub>3</sub>	60	1067 (0.2 C)	780 (2 C)	0.25 (0.2 C, 100 cycles)	5
PAA-SWNT/Celgard <sup>b</sup>	65	1130 (0.1 C)	592 (2 C)	0.13 (1 C, 200 cycles)	6
COF@CNT/Celgard <sup>c</sup>	75	1130 (0.2 C)	600 (10 C)	0.05 (2 C, 300 cycles)	7
PAA/Celgard <sup>d</sup>	70	713 (0.1 C)	373 (2 C)	0.07 (0.5 C, 600 cycles)	8
GO membrane/Celgard	63	920 (0.1 C)	580 (2 C)	0.26 (0.1 C, 100 cycles)	9
<b>E-PAN/PAA</b>	<b>60</b>	<b>1232 (0.1 C)</b>	<b>563 (2 C)</b>	<b>0.03 (1 C, 500 cycles)</b>	<b>This work</b>

KB@Ir/Celgard <sup>a</sup>: Ketchen Black and Ir nanoparticle modified Celgard.

PAA-SWNT/Celgard <sup>b</sup>: Poly(acrylic acid) coated single-walled carbon nanotube film on Celgard.

COF@CNT/Celgard <sup>c</sup>: Microporous covalent organic framework (COF) net and mesoporous carbon nanotube (CNT) net modified Celgard.

PAA/Celgard <sup>d</sup>: Poly(acrylic acid) modified Celgard.

## References

1. Z. A. Ghazi, X. He, A. M. Khattak, N. A. Khan, B. Liang, A. Iqbal, J. X. Wang, H. Sin, L. S. Li and Z. Y. Tang, *Adv. Mater.*, 2017, **29**, 1606817.
2. J. Sun, Y. M. Sun, M. Pasta, G. M. Zhou, Y. Z. Li, W. Liu, F. Xiong and Y. Cui, *Adv. Mater.*, 2016, **28**, 9797-9803.
3. P. J. Zuo, J. F. Hua, M. X. He, H. Zhang, Z. Y. Qian, Y. L. Ma, C. Y. Du, X. Q. Cheng, Y. Z. Gao and G. P. Yin, *J. Mater. Chem. A*, 2017, **5**, 10936-10945.
4. Z. Li, Y. Han, J. H. Wei, W. Q. Wang, T. T. Cao, S. M. Xu and Z. H. Xu, *ACS Appl. Mater. Interfaces*, 2017, **9**, 44776-44781.
5. R. S. Song, R. P. Fang, L. Wen, Y. Shi, S. G. Wang and F. Li, *J. Power Sources*, 2016, **301**, 179-186.
6. J. H. Kim, J. Seo, J. Choi, D. Shin, M. Carter, Y. Jeon, C. W. Wang, L. B. Hu and U. Paik, *ACS Appl. Mater. Interfaces*, 2016, **8**, 20092-20099.
7. J. T. Yoo, S. J. Cho, G. Y. Jung, S. H. Kim, K. H. Choi, J. H. Kim, C. K. Lee, S. K. Kwak and S. Y. Lee, *Nano Lett.*, 2016, **16**, 3292-3300.
8. S. L. Song, L. Shi, S. Y. Lu, Y. C. Pang, Y. K. Wang, M. Zhu, D. W. Ding and S. J. Ding, *J. Membr. Sci.*, 2018, **563**, 277-283.
9. J. Q. Huang, T. Z. Zhuang, Q. Zhang, H. J. Peng, C. M. Chen and F. Wei, *ACS Nano*, 2015, **9**, 3002-3011.